

Possibility of Spinodal Decomposition in ZrO_2 - Y_2O_3 Alloys: A Theoretical Investigation

Danan Fan* and Long-Qing Chen*

Department of Materials Science and Engineering, The Pennsylvania State University,
University Park, Pennsylvania 16802

The thermodynamics and kinetics of cubic \rightarrow tetragonal phase transformations in ZrO_2 - Y_2O_3 alloys were investigated by using thermodynamic stability analysis and kinetic computer simulations to explore the possibility of a spinodal mechanism during decomposition. Based on a simple free energy model, it is shown that, depending on the alloy composition, a cubic phase aged within the $t + c$ two-phase field may result in three different sequences of phase transformations: (1) direct nucleation and growth of the equilibrium t -phase from the c -phase matrix; (2) formation of a metastable t' -phase followed by nucleation and growth of the equilibrium c - and t -phases; and (3) formation of a transient t' -phase followed by its spinodal decomposition into two tetragonal phases with one of the tetragonal phases eventually transforming to the equilibrium c -phase. The temporal microstructure evolutions for different compositions were studied by using computer simulations based on the time-dependent Ginzburg-Landau (TDGL) model which incorporates the long-range elastic interactions.

I. Introduction

THE discovery of the transformation-toughening behavior in partially stabilized zirconia (PSZ) has generated enormous interest in the phase transformation behaviors of ZrO_2 - Y_2O_3 alloys in the last two decades.^{1,2} In particular, the cubic (c) ZrO_2 to tetragonal (t) ZrO_2 transformation has been extensively studied³⁻⁸ since the shape, size, and spatial distribution of the tetragonal particles strongly affect the mechanical properties of the material.

A c -phase in the ZrO_2 - Y_2O_3 system may transform to a t -phase by either a diffusional or a diffusionless transformation. A diffusionless and displacive transformation results in the formation of so-called t' -phase,⁹ i.e., a t -phase with the same concentration as the original c -phase. It was found that this transformation always goes to completion in quenched alloys or in arc-melted and subsequently quenched alloys.^{9,10} If a quenched alloy is aged in the $c + t$ two-phase region, or if an alloy is cooled slowly through the two-phase region, precipitation of the t -phase occurs by a diffusional decomposition. Transmission electron microscopy (TEM) observations of the decomposed microstructure sometimes show a characteristic image contrast consisting of fine striations,^{3,10,11} and in other cases, the formation of modulated structures.¹⁰⁻¹⁴

To explain the origin of the image contrast and the modulated structure, two conflicting interpretations have been proposed. One suggests that the decomposition of the original c -phase or the intermediate t' -phase is a process of nucleation and growth of fine t -phase particles, and the image contrast observed under

TEM arises from the strain fields around those particles.³ The other suggests that spinodal decomposition is responsible for the image contrast and the formation of modulated structures.¹⁰⁻¹³

Current knowledge on the decomposition mechanism is still insufficient to reach a conclusion on the argument. Most of the disagreement concerns the following three questions: (1) Is spinodal decomposition possible in the ZrO_2 - Y_2O_3 system? (2) Are the experimentally observed modulated structures due to spinodal decomposition? (3) If spinodal decomposition does occur in the ZrO_2 - Y_2O_3 system, does it occur in the c -phase, or in the t' -phase?

The main objective of this paper is to address some of these questions by combining thermodynamic stability analysis and kinetic computer simulations of microstructure evolution based on the time-dependent Ginzburg-Landau (TDGL) model.

II. Thermodynamic Model for the ZrO_2 - Y_2O_3 System

Previous thermodynamic models treated the $c \rightarrow t$ phase transformation in the ZrO_2 - Y_2O_3 system as a second-order phase transformation,^{15,16} in which the free energy versus composition curve of the t -phase is assumed to be a continuous branch of the c -phase. However, it is generally believed that the $c \rightarrow t$ transformation in ZrO_2 is first-order^{3,9} and that the c - and t -phases have two different free energy curves.⁹ Furthermore, even if the $c \rightarrow t$ transformation is second-order in pure ZrO_2 , it would soon become first-order when oxides like Y_2O_3 and MgO are added into ZrO_2 .¹⁵ Therefore, in this work the $c \rightarrow t$ phase transformation in the Y_2O_3 - ZrO_2 system is treated as first-order.

In order to describe the free energies of both parent and product phases in a structural transformation with symmetry changes within the same physical and mathematical model, one needs to introduce order parameter fields or phase-fields, $\eta_i(\mathbf{r})$ ($i = 1, 2, 3, \dots, \nu$, where ν is the number of order parameters). In a $c \rightarrow t$ transformation, the number of different orientation variants dictated by the crystal symmetry is three, with the tetragonal axes along crystallographic directions [100], [010], and [001] of the parent cubic phase. For a phase decomposition, a continuous field of composition, $c(\mathbf{r})$, also needs to be defined.

In this paper, the local specific chemical free energy of the ZrO_2 - Y_2O_3 system at a given temperature is approximated by the following Landau free energy polynomial:

$$\begin{aligned}
 f(c, \eta_1, \eta_2, \eta_3) = & \frac{1}{2}A(c - c_1)^2 + \frac{1}{2}B(c - c_2) \left(\sum_{i=1}^3 \eta_i^2 \right) \\
 & - \frac{1}{4}D \left(\sum_{i=1}^3 \eta_i^4 \right) + \frac{1}{6}G \left(\sum_{i=1}^3 \eta_i^6 \right) + U \left(\sum_{i \neq j}^3 \eta_i^2 \eta_j^2 \right) \\
 & + V \left(\sum_{i \neq j \neq k}^3 \eta_i^4 [\eta_j^2 + \eta_k^2] \right) + W(\eta_1^2 \eta_2^2 \eta_3^2)
 \end{aligned}
 \tag{1}$$

where c is composition, η_1 , η_2 , and η_3 are order parameters

A. V. Virkar—contributing editor

Manuscript No. 193263. Received August 30, 1994; approved January 23, 1995.
Supported by the National Science Foundation under Grant No. NSF-93-11898.
*Member, American Ceramic Society.

characterizing the amplitudes of the displacive modes of the $c \rightarrow t$ transformation or the symmetry difference between the c - and t -phases, $A, B, D, G, U, V,$ and W are positive phenomenological constants, c_1 is determined by the equilibrium composition of the c -phase, and c_2 is a constant beyond which the cubic phase is unstable with respect to its transformation to the t -phase.

Equation (1) defines a hypersurface of the specific chemical free energy, f , in a four-dimensional phase-space formed by c and the three order parameters, η_i . The free energy of the c -phase as a function of composition is obtained by setting all the order parameters equal to zero. The free energy of the t -phase is obtained as follows: first, minimize the free energy with respect to a given order parameter η_i at a given c , under the condition that two other order parameters are zero; second, find the equilibrium order parameter at a fixed composition; and finally, substitute the equilibrium order parameter, which is a function of composition, back into the original free energy function to obtain the free energy of the t -phase. Therefore, the free energy of the t -phase as a function of composition is actually the trajectory of projected free energy minima with respect to η_i on the f - c plane.

It is emphasized that the main interest of this study is to explore the possibility of spinodal decomposition and the microstructure evolution in the ZrO_2 - Y_2O_3 system. The units of the coefficients and the exact value of the free energy are not very important as long as they provide the correct free energy topology in the composition and order parameter space. In this work those constants are chosen as $A = 2.0, B = 1.1, D = 0.1, G = 1.5, U = 2.0,$ and $V = W = 1.0$, which provide equilibrium composition for the t -phase, $c_{tet} = 2.4$ (mol%), and for the c -phase, $c_{cub} = 8.1$ (mol%), which are close to the equilibrium compositions of Y_2O_3 - ZrO_2 at $1500^\circ C$.^{3,4} These coefficients have been chosen rather arbitrarily and many other sets of parameter values are possible. The justification is based on our argument that as long as they provide similar free energy curves for c - and t -phases as a function of composition, they will result in similar transformation kinetics.

The free energy versus composition curves for the c - and t -phases calculated from Eq. (1) are shown in Fig. 1, which shows a first-order transition and a spinodal region in the t -phase. In Fig. 1, c_s is the composition at which the second-derivative of the free energy of the t -phase with respect to composition is equal to zero, i.e., the spinodal point; c_- is the composition below which the c -phase is absolutely unstable with respect to the t -phase, c_0 is the composition at which the free energies of the t - and c -phases are equal, and c_+ is the composition above which the t -phase becomes absolutely unstable with respect to the c -phase.

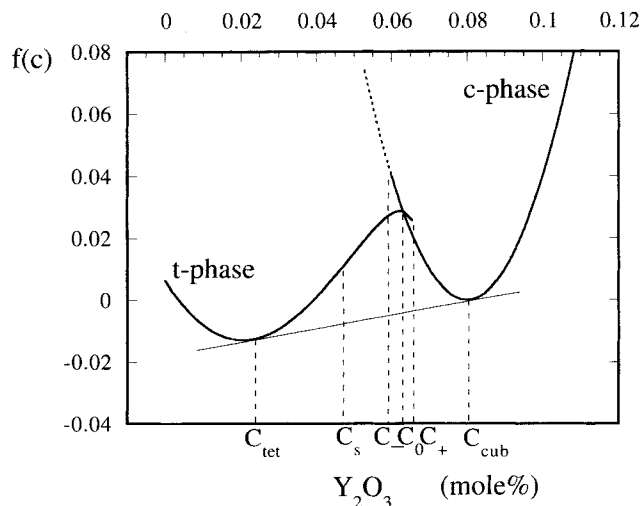


Fig. 1. Specific free-energy vs composition curves for both the cubic and tetragonal phases calculated according to Eq. (1) with $A = 2.0, B = 1.1, D = 0.1, G = 1.5, U = 2.0,$ and $V = W = 1.0$. See text for explanation.

III. Thermodynamic Stability Analysis

Thermodynamic stability analysis combined with some simple kinetic arguments have proved to be a very powerful tool in the qualitative understanding of the kinetics of phase transformations in metallic alloy systems in which both ordering and phase separation are involved.¹⁷⁻¹⁹ In the ZrO_2 - Y_2O_3 system, simultaneous displacive and diffusional transformations take place, and the displacive transformation which requires only concerted displacements of atoms occurs much faster than phase decomposition which requires long-range diffusion with a diffusion distance on the order of the size of second-phase precipitates or typical microstructure scales. Therefore, if there is a possibility of reducing the system free energy through a displacive transformation, it should take place first. With this rule in mind and with the simple free energy model (Eq. (1), Fig. 1) proposed for the ZrO_2 - Y_2O_3 system, then in the case of a c -phase aged within the $t \rightarrow c$ two-phase field, the following phase transformation scenarios are possible:

(1) $c_{tet} < c < c_s$

A c -phase within this composition range is absolutely unstable with respect to its transformation into the t -phase. Hence, the first stage of the transformation during aging involves a continuous displacive transformation which results in an intermediate t' -phase with the same composition as the original c -phase. The driving force for this process is the difference between free energies of the c -phase and t -phase at the same composition (it is t' -phase, Figs. 1 and 2). From Figs. 1 and 2, a t' -phase within this composition range is metastable with respect to the formation of the equilibrium c -phase with composition c_{cub} . Therefore, the second stage of transformation is the nucleation and growth of the equilibrium c -phase from the t' -phase, producing the equilibrium $c + t$ two-phase mixture. The driving force for the second stage is the difference between the free energies of the t' -phase and the equilibrium $c + t$ two-phase mixture (Figs. 1 and 2).

(2) $c_s < c < c_0$

We can subdivide this composition range into two parts, $c_s < c < c_-$ and $c_- < c < c_0$. Within the composition range $c_s < c < c_-$, the initial c -phase is unstable with respect to the continuous transformation into the t' -phase with the same composition through a displacive transformation. Different from case (1), the free energy of the t' -phase within this composition range has a negative curvature (Fig. 1), and therefore a spinodal mechanism is expected for the decomposition of the t' -phase. Initial spinodal decomposition of the t' -phase will result in two tetragonal phases with different compositions. One

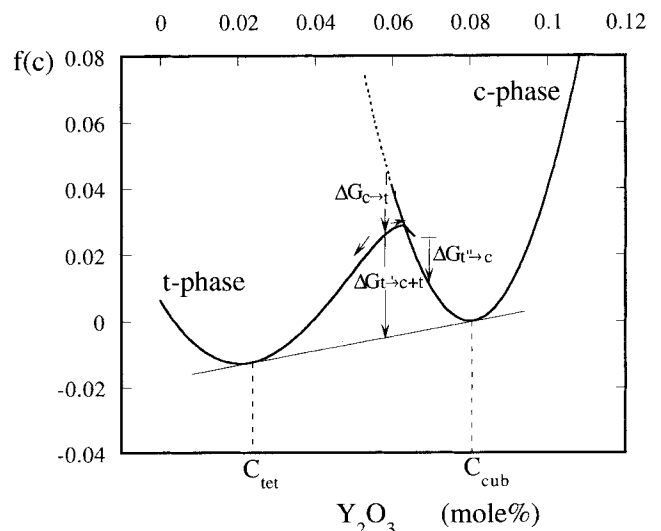


Fig. 2. Schematic phase transformation path for a cubic phase within the composition range $c_s < C < c_-$.

of the tetragonal phases will become the equilibrium t-phase as its composition reaches c_{tet} whereas the other tetragonal phase will continue to increase its composition until c_+ , beyond which it spontaneously transforms to the c-phase. The final equilibrium state is again the c + t two-phase mixture. The schematic transformation path for this composition range is shown in Fig. 2, in which $\Delta G_{c \rightarrow t}$, $\Delta G_{t \rightarrow c+t}$, and $\Delta G_{t \rightarrow c}$ are the driving forces for the $c \rightarrow t'$ displacive transformation, for the spinodal decomposition of the t' -phase into a two-phase mixture of c + t phases, and for the Y_2O_3 -rich t-phase transforming to the c-phase, respectively.

Within the composition range $c_- < c < c_0$, the initial c-phase is metastable. Therefore, $c \rightarrow t'$ displacive transformation occurs through a nucleation and growth process. However, since the free energy of the t' -phase is lower than that of the c-phase at the same composition, the transformation may be a massive transformation because the rate of displacive transformation is much faster than decomposition. The intermediate t' -phase is again unstable with respect to infinitesimal composition fluctuations and its decomposition into the equilibrium c + t two-phase mixture takes place through a spinodal mechanism followed by a $t \rightarrow c$ transformation in the Y_2O_3 -rich tetragonal phase.

(3) $c > c_0$

A cubic phase within this composition range is metastable with respect to the formation of the t-phase. Moreover, the free energy of the t-phase is higher than that of the c-phase. Therefore, the t-phase will precipitate directly from the c-phase through a nucleation and growth process without undergoing an intermediate $c \rightarrow t'$ transformation.

IV. TDGL Kinetic Model

The thermodynamic stability analysis based on free energy versus composition curves (as discussed above) provides an elegant way of qualitatively understanding the phase transformation sequence. However, the actual kinetics of phase transformation and, in particular, the microstructure evolution during phase transformations have to be investigated by using kinetic models. In this paper we employ the TDGL kinetic model in which the microstructure evolution is modeled by the temporal and spatial evolution of order parameter fields and composition fields toward equilibrium.^{20–23} A computer simulation based on the TDGL model involves a numerical solution of the coupled Cahn–Allen²⁵ and Cahn–Hilliard² equations:

$$\frac{\partial \eta_i(\mathbf{r}, t)}{\partial t} = -L \frac{\delta F}{\delta \eta_i(\mathbf{r}, t)} + \xi_i(\mathbf{r}, t) \quad (2a)$$

$$\frac{\partial c(\mathbf{r}, t)}{\partial t} = M \nabla^2 \frac{\delta F}{\delta c(\mathbf{r}, t)} + \xi_c(\mathbf{r}, t) \quad (2b)$$

where L and M are kinetic coefficients which characterize the interface mobility and atomic diffusivity, respectively. F is the total free energy expressed in the unit of $k_B T$, where k_B is the Boltzmann constant and T is the temperature. ξ_c and ξ_i are the Langevin random noise terms which describe the thermal fluctuation of concentration and order parameters, respectively. They are assumed to be Gaussian-distributed and obey the fluctuation–dissipation relations:

$$\langle \xi_i(\mathbf{r}_1, t_1) \xi_j(\mathbf{r}_2, t_2) \rangle = 2k_B T L \delta(t_2 - t_1) \delta(\mathbf{r}_2 - \mathbf{r}_1) \delta_{ij} \quad (3a)$$

$$\langle \xi_c(\mathbf{r}_1, t_1) \xi_c(\mathbf{r}_2, t_2) \rangle = -2k_B T M \nabla^2 \delta(t_2 - t_1) \delta(\mathbf{r}_2 - \mathbf{r}_1) \quad (3b)$$

In a structural transformation, the total nonequilibrium free energy F contains both the “chemical” free energy F_c and the strain energy E . The chemical free energy is associated with the finite-range interatomic interaction and, according to the diffuse interface theory of Cahn and Hilliard,²⁴ can be written as

$$F_c = \int_V \left[\frac{1}{2} \alpha |\nabla c|^2 + \frac{1}{2} \beta \left(\sum_{i=1}^p |\nabla \eta_i|^2 \right) + f(c, \eta_1, \eta_2, \dots, \eta_p) \right] dv \quad (4)$$

where α and β are gradient energy coefficients for concentration and order parameters, respectively, and f is the local free energy density (Eq. (1)).

According to the linear elasticity theory of Khachatryan^{26,27} and recent work on diffuse interfaces,^{20–23} the local stress-free transformation strain $\varepsilon_{ij}^{\circ}(p)$, during a decomposition phase transformation, is related to continuous order parameter fields through

$$\varepsilon_{ij}^{\circ}(\mathbf{r}) = \sum_{p=1}^q \varepsilon_{ij}^{\circ\circ}(p) \eta_p^2(\mathbf{r}) \quad (5)$$

where $\varepsilon_{ij}^{\circ\circ}(p)$ and $\eta_p(\mathbf{r})$ are the proportionality constant and the local order parameter field for a particular variant p . The total strain energy E induced by an arbitrary distribution of coherent second-phase particles can be expressed as^{23,26,27}

$$E = E^{\text{inc}} + E^{\text{hom}} + E^{\text{het}} \quad (6)$$

here E^{inc} is the elastic energy increase, E^{hom} is the relaxation energy with respect to the homogeneous strain, and E^{het} is the relaxation energy with respect to the heterogeneous strain; and

$$E^{\text{inc}} = \frac{1}{2} \int_V \lambda_{ijkl} \sum_{p=1}^3 \varepsilon_{ij}^{\circ\circ}(p) \varepsilon_{kl}^{\circ\circ}(p) \eta_p^4(\mathbf{r}) d^3r \quad (6a)$$

$$E^{\text{hom}} = -\frac{1}{2V} \sum_{p=1}^3 \sum_{q=1}^3 \lambda_{ijkl} \varepsilon_{ij}^{\circ\circ}(p) \varepsilon_{kl}^{\circ\circ}(q) \int_V \eta_p^2(\mathbf{r}) d^3r \times \int_V \eta_q^2(\mathbf{r}') d^3r' \quad (6b)$$

$$E^{\text{het}} = -\frac{1}{2} \sum_{p=1}^3 \sum_{q=1}^3 \int \left(\frac{d^3k}{(2\pi)^3} [n_i \sigma_{ij}^{\circ}(p) \Omega_{jk}(\mathbf{n}) \sigma_{kl}^{\circ}(q) n_l] \cdot \{ \eta_p(\mathbf{r}^2) \}_k \{ \eta_q(\mathbf{r}^2) \}_k^* \right) \quad (6c)$$

where λ_{ijkl} is the elastic modulus tensor, $\sigma_{ij}^{\circ}(p) = \lambda_{ijkl} \varepsilon_{kl}^{\circ\circ}(p)$, \mathbf{k} is a wave vector in the reciprocal space, $n_i = k_i/k$ is the i th component of a unit vector parallel to \mathbf{k} , $\Omega_{jk}(\mathbf{n})$ is a Green function matrix reciprocal to $\Omega_{jk}^{-1} = \lambda_{ijkl} n_i n_l$, and

$$\{ \eta_p^2(\mathbf{r}) \}_k = \int_V \eta_p^2(\mathbf{r}) \exp(-i\mathbf{k} \cdot \mathbf{r}) d^3r \quad (7)$$

$\{ \eta_q(\mathbf{r}^2) \}_k^*$ is the complex conjugate of $\{ \eta_q(\mathbf{r}^2) \}_k$. The integrations are taken over the system volume V and the singular branching point $\mathbf{k} = 0$ is excluded from the integration in Eq. (6c). If homogeneous strain relaxation is not allowed, such as in the case of a crystalline grain constrained by neighboring grains, E^{hom} is equal to zero.

For a $c \rightarrow t$ phase transformation, $\varepsilon_{ij}^{\circ\circ}(p)$ can be written as

$$\varepsilon_{ij}^{\circ\circ}(1) = \begin{vmatrix} \varepsilon_{33}^{\circ} & 0 & 0 \\ 0 & \varepsilon_{11}^{\circ} & 0 \\ 0 & 0 & \varepsilon_{11}^{\circ} \end{vmatrix} \quad (8a)$$

$$\varepsilon_{ij}^{\circ\circ}(2) = \begin{vmatrix} \varepsilon_{11}^{\circ} & 0 & 0 \\ 0 & \varepsilon_{33}^{\circ} & 0 \\ 0 & 0 & \varepsilon_{11}^{\circ} \end{vmatrix} \quad (8b)$$

$$\varepsilon_{ij}^{\circ\circ}(3) = \begin{vmatrix} \varepsilon_{11}^{\circ} & 0 & 0 \\ 0 & \varepsilon_{11}^{\circ} & 0 \\ 0 & 0 & \varepsilon_{33}^{\circ} \end{vmatrix} \quad (8c)$$

where $\epsilon_{11}^o = (a_t - a_c)/a_c$, $\epsilon_{33}^{oo} = (c_t - a_c)/a_c$, a_c is the lattice parameter of c- ZrO_2 , and a_t and c_t are the lattice parameters of t- ZrO_2 in the ZrO_2 - Y_2O_3 system.

The total free energy including the transformation-induced strain energy can then be written as

$$F = F_c + \kappa E \quad (9)$$

where F_c and E are calculated from Eqs. (4) and (6), respectively. κ is a coefficient related to the contribution of elastic energy to the total free energy of the system.

V. Computer Simulations

Because of the extensive computation involved in a three-dimensional (3D) kinetic study, we employed a two-dimensional (2D) system which can be viewed as the projection from a 3D system. In the computer simulation, a square cell with 256×256 grids is employed with periodic boundary conditions along both x and y directions. TDGL equations are solved in the reciprocal space using explicit forward Euler equations.

The experimental data for the elastic constants of Y_2O_3 - ZrO_2 are $c_{11} = 3.94 \times 10^{11}$ Pa, $c_{12} = 0.91 \times 10^{11}$ Pa, and $c_{44} = 0.56 \times 10^{11}$ Pa as given in Ref. 6; and lattice parameters, $a_c = 5.128$ Å, $a_t = 5.090$ Å, and $c_t = 5.180$ Å, are taken from Ref. 3. All of the energies involved in the numerical calculation are measured in units of $k_B T \cong 2 \times 10^8$ J/m³. Reduced time t^* is used in the simulation, which is defined as $t^* = t/t_0$, $t_0 = (Lk_B T)^{-1}$. The elastic energy coefficient κ is chosen to be 0.04. Since the information about the interfacial energy in Y_2O_3 - ZrO_2 alloys is not available, it was rather arbitrarily assumed that the gradient energy coefficients α and β in Eq. (3) are 3.0.

Two alloys with $c = 4.2$ mol% (alloy 1) and 5.6 mol% (alloy 2) are chosen for computer simulations. As indicated in Fig. 2, the compositions of alloys 1 and 2 are within the composition ranges $c_{tet} - c_s$ and $c_s - c_0$, respectively. According to the thermodynamic stability analysis discussed above, aging of a cubic phase of alloy 1 or alloy 2 always undergoes a $c \rightarrow t'$ transformation before decomposition into the equilibrium $c + t$ two-phase mixture occurs.

Since the rate of displacive $c \rightarrow t'$ transformation is much (orders of magnitude) faster than the $t' \rightarrow c + t$ decomposition process, simulations were divided into two steps. The first step was that M was set to zero in Eq. (2b) to simulate the displacive $c \rightarrow t'$ transformation ($M/L = 0$, without any diffusion). After the displacive transformation is completed, the decomposition of t' -phase was simulated within a single t' variant and $M/L = 0.2$ was chosen for Eqs. (2a) and (2b). Other ratios for M/L may be used and the results will essentially be the same as long as they provide faster relaxation kinetics for the order parameters than the redistribution of composition. This treatment is also based on the experimental fact that $c \rightarrow t'$ transformation completes before any significant diffusion occurs.^{9,13}

The detailed kinetics of tweed and twin formation during the $c \rightarrow t'$ transformation have been discussed in a separate publication.²³ An example of the microstructure evolution during a $c \rightarrow t'$ displacive transformation in alloy 2 ($c = 5.6$ mol%) predicted from our computer simulation with $M = 0$ is shown in Fig. 3. In Fig. 3, the gray levels represent the magnitudes of the square of one of the order parameters, and therefore white regions are domains belonging to one of the t' -phase variants and dark regions are those belonging to the other variant. It can be seen that $c \rightarrow t'$ displacive transformation reaches completion rapidly (Fig. 3(a)) and results in the formation of anti-phase domain boundaries within the tweed and twin structure (Fig. 3(d)). Since $c \rightarrow t'$ displacive transformation always goes to completion before decomposition occurs, the initial condition was chosen to be a homogeneous t' -phase single-domain instead of a cubic phase in the second step.

(1) Alloy 1

The initial state of alloy 1 is a uniform t' -phase single-domain with tetragonality along the x -direction (labeled as 1) generated

by assigning $c = 4.2$ mol%, $\eta_2 = 0$ everywhere, and $\eta_1 = \eta_1(c)$, where $\eta_1(c)$ is the equilibrium value of the order parameter, η_1 , at a fixed composition c . As discussed in the thermodynamic analysis, the t' -phase at this composition is metastable with respect to the formation of the c -phase. Indeed, the computer simulation showed small initial random perturbations to the uniform composition decay. Therefore, thermal noise terms are required in the initial stage to produce nuclei of the c -phase. The noise terms are turned off after nucleation.

The morphological evolution of concentration fields during decomposition for alloy 1 is shown in Fig. 4, in which the local compositions, $c(r)$, are represented by gray levels. The brighter the color, the higher the composition. Therefore, the brighter regions are c -phase domains and dark regions are t -phase domains. As can be seen from Fig. 4, there is no gradual development of concentration waves typical of spinodal decomposition. Instead, local regions with large composition fluctuations and with sizes larger than that of the critical nucleus transformed to the c -phase. Nevertheless, during growth of the c - and t -phase and during coarsening, the elastic energy arising from lattice mismatch between the c - and t -phases results in the alignment of precipitates along the elastic soft directions ($\langle 11 \rangle$) (Figs. 4(b-d)).

(2) Alloy 2

The initial condition for alloy 2 is similar to alloy 1, i.e., a uniform composition ($c = 5.6$ mol%) and a uniform order parameter ($\eta_1 = \eta_1(c)$ and $\eta_2 = 0$). Different from alloy 1, however, small random perturbations to the uniform composition result in the gradual development of basket-weave type composition modulations (Fig. 5(a)). By comparing Figs. 5 and 4, the difference is quite obvious. In alloy 1, the initial stage involves direct nucleation of the c -phase particles from the t' -phase, whereas in alloy 2, initial decomposition results in two tetragonal phases with different compositions (Fig. 5(a)). Later, the Y_2O_3 -rich tetragonal phase transforms to the c -phase (Fig. 5(b)). Figures 5(b) to (d) demonstrate the coarsening process of the $c + t$ two-phase microstructure, during which the wavelength of concentration increases. The modulated structures in Fig. 5 are very similar to those obtained from TEM observations.¹⁰⁻¹⁴

The degree of microstructure alignment and the shapes of tetragonal particles depend on both the elastic energy generated during the transformation and the interfacial energy determined by the gradient energy coefficients. The fact that the composition modulation is strongly aligned indicates the microstructure evolution of the $c + t$ two-phase mixture is mainly controlled by the elastic strain energy. As a comparison, the microstructure evolution for a system with a lower elastic energy contribution ($\kappa = 0.01$) is shown in Figs. 6 and 7 for compositions $c = 4.2$ and 5.6 mol%, respectively. It is quite obvious that the alignments in Figs. 6 and 7 are weaker than those in Figs. 4 and 5.

From Fig. 5 and 7 it is shown that the direction of composition modulation developed during spinodal decomposition and coarsening is perpendicular to the $\langle 11 \rangle$ directions, which are elastic soft directions in this 2D simulation. To predict if the composition modulation is perpendicular to the $\langle 111 \rangle$ direction in three dimensions, 3D computer simulations are required.

VI. Discussion

Different schematic free energy models for the c -phase and t -phase have been previously proposed in order to explain the experimental observations of microstructure evolution in ZrO_2 - Y_2O_3 alloys. For example, based on free energy curves similar to those shown in Fig. 8(a), Heuer *et al.*³ interpreted that aging a c -phase within the $c + t$ two-phase field results in the direct nucleation and growth of t -phase particles from the c -phase matrix. Another explanation for the modulated structures is the result of a spinodal decomposition. It was initially thought that it is most probable to have a spinodal region present in c -phase¹²

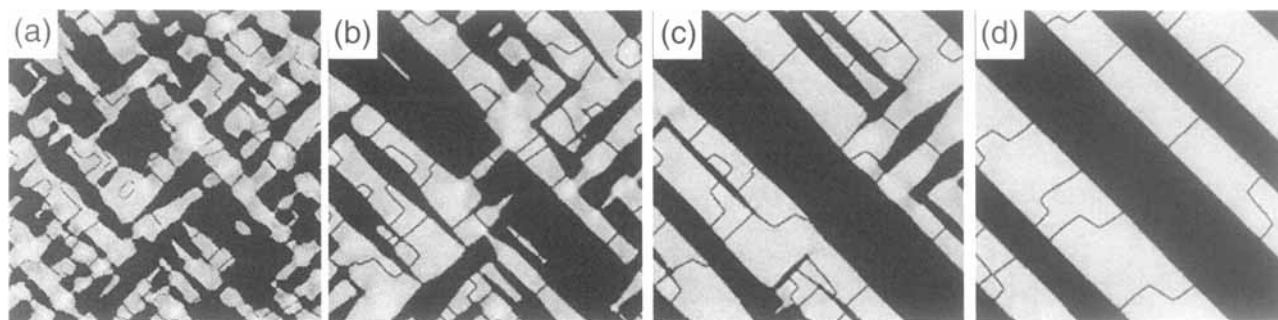


Fig. 3. Temporal evolution of order parameter fields during $c \rightarrow t'$ transition in alloy 2 ($c = 5.6$ mol%): (a) η_1 field at $t^* = 0.2$, (b) η_1 field at $t^* = 1.0$, (c) η_1 field at $t^* = 2.0$, (d) η_1 field at $t^* = 3.0$.

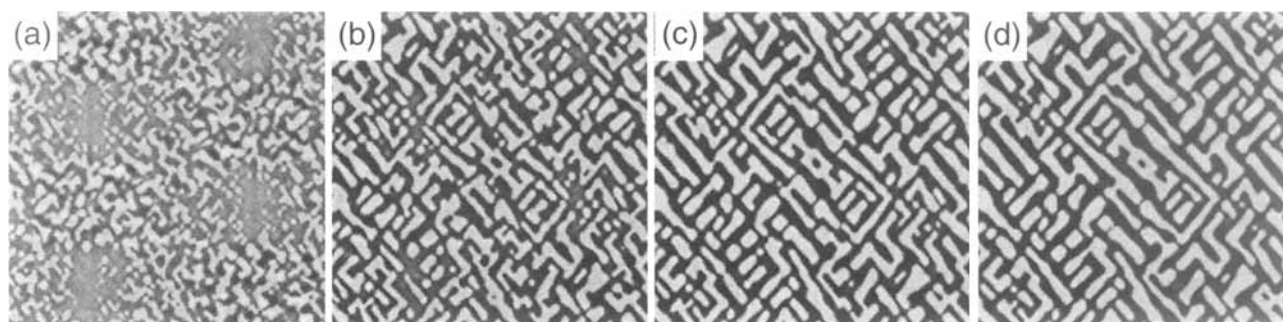


Fig. 4. Temporal evolution of concentration field during decomposition of a single t' -phase domain in alloy 1 ($c = 4.2$ mol%, $\kappa = 0.04$): (a) $t^* = 0.05$, (b) $t^* = 0.3$, (c) $t^* = 0.7$, (d) $t^* = 1.0$.

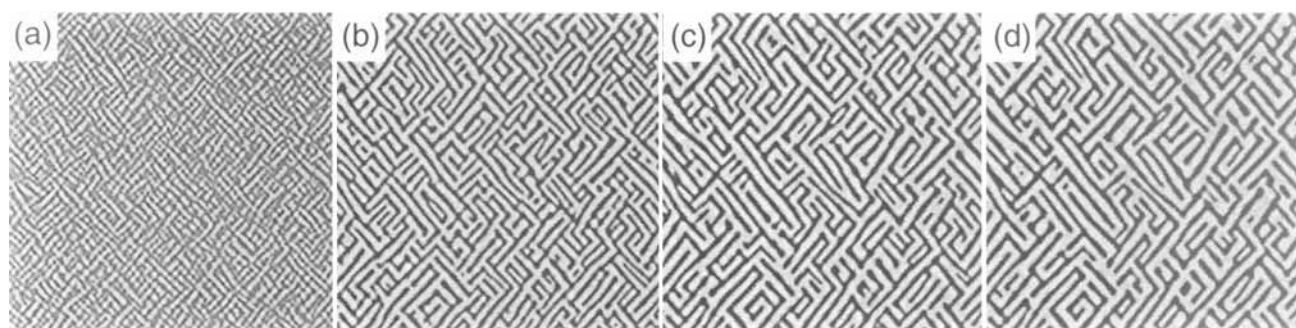


Fig. 5. Temporal evolution of concentration field during decomposition of a single t' -phase domain in alloy 2 ($c = 5.6$ mol%, $\kappa = 0.04$): (a) $t^* = 0.05$, (b) $t^* = 0.3$, (c) $t^* = 0.7$, (d) $t^* = 1.0$.

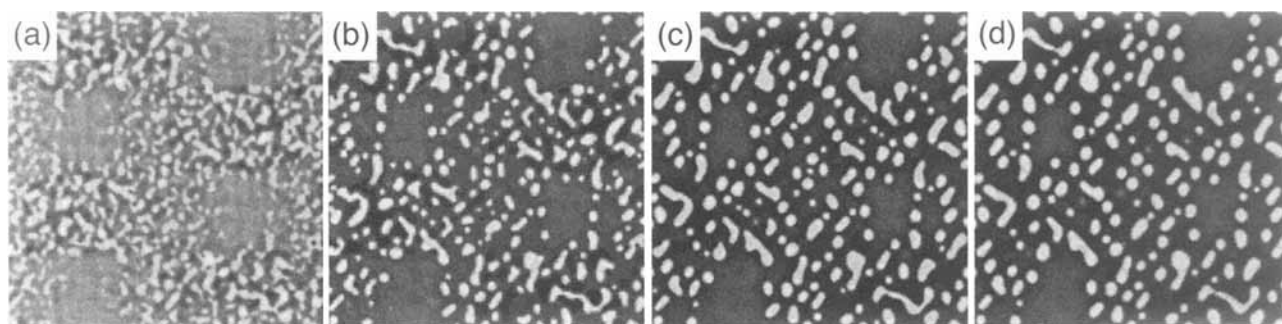


Fig. 6. Temporal evolution of concentration field during decomposition of a single t' -phase domain in alloy 1 ($c = 4.2$ mol%, $\kappa = 0.01$): (a) $t^* = 0.05$, (b) $t^* = 0.3$, (c) $t^* = 0.7$, (d) $t^* = 1.0$.

as shown in Fig. 8(b). However, Sakuma *et al.* argued that this interpretation cannot explain the appearance of electron reflections which always correspond to the t -phase.¹² Therefore, Sakuma *et al.* proposed another set of free energy curves as shown in Fig. 8(c), in which the free energies of the t -phase and c -phase were continuous,^{12,13} which requires that the $c \rightarrow t$

transformation be second-order and that the lattice parameter change continuously from c -phase to t -phase as the composition changes.

The free energy curves in our model are schematically redrawn in Fig. 8(d) with the width of the spinodal region exaggerated for the purpose of clarity. Figure 8(d) is similar to

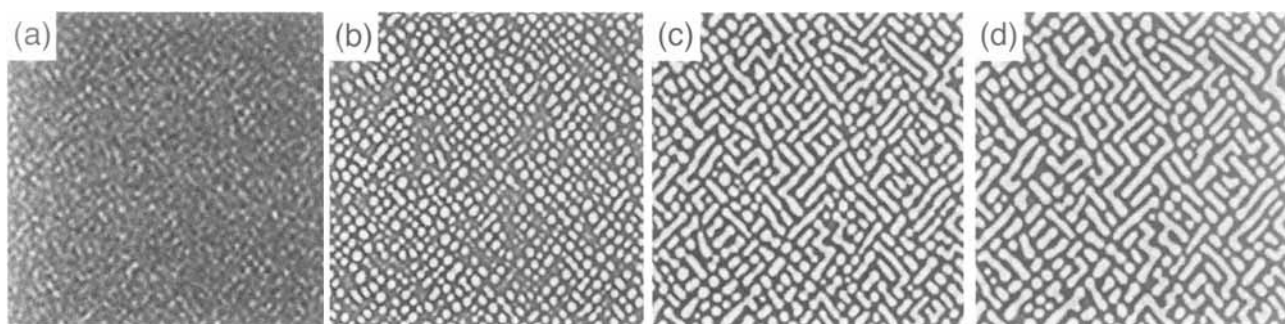


Fig. 7. Temporal evolution of concentration field during decomposition of a single t' -phase domain in alloy 2 ($c = 5.6$ mol%), $\kappa = 0.01$: (a) $t^* = 0.05$, (b) $t^* = 0.3$, (c) $t^* = 0.7$, (d) $t^* = 1.0$.

Fig. 8(c) with the important exception that there are two separate free energy curves for c-phase and t-phase, respectively, in Fig. 8(d), indicating a first-order $c \rightarrow t$ phase transformation and a discontinuous lattice parameter change. Moreover, our interpretation of the transformation sequence is different from previous works.¹¹⁻¹³ We employ a kinetic argument: displacive transformation which does not involve atomic diffusion occurs much faster than phase separation which requires long-distance diffusion. On the basis of this argument, we claim that as long as there is a segment of the free energy curve of the t-phase which has a negative second derivative with respect to composition and whose values are lower than those of the c-phase, a quenched c-phase aged within the $c + t$ phase field will result in the displacive $c \rightarrow t'$ transformation followed by the spinodal decomposition of the t' -phase into two tetragonal phases (Fig. 2). One of the tetragonal phases resulting from the spinodal decomposition will eventually transform to the c-phase (Fig. 2). In other words, during aging of a c-phase within the two-phase field, spinodal decomposition will take place, but under the condition that a $c \rightarrow t$ displacive transformation occurs first. Such a spinodal is called "conditional spinodal" in the metallurgical literature and is very common in alloy systems in which simultaneous ordering and phase separation take

place.¹⁷⁻¹⁹ The phase transformation path predicted in our model is consistent with the observations of electron reflections from modulated structures.¹² A crucial test if spinodal decomposition occurs in the t' -phase is whether or not two tetragonal phases with different compositions are observed in the initial stages of decomposition (Fig. 5(a)). Recent work^{10,13} seems to show that the modulated structure is generated from fully tetragonal structure and the modulated structures are made up of two tetragonal phases with different compositions in the initial stages of decomposition.¹⁰

In comparing our theoretical predictions with experimental observations, it is noted that the composition range within which Sakuma *et al.*¹¹ claimed spinodal decomposition occurs is considerably wider than that predicted in our free energy model. There are two aspects that need to be discussed. First, Sakuma *et al.*¹² determined the spinodal region based on their observation that modulated structures of alternating c- and t-phases exist after an alloy is aged within the $c + t$ two-phase field for a long time. From our computer simulations, modulated structures can also form during nucleation and growth (Fig. 4). The formation of modulated structures is mainly due to the strain-induced coarsening. Moreover, Heuer *et al.*³ did not find any strong evidence for spinodal decomposition such as the gradual development of composition modulations. Therefore, experimentally, the composition range in which spinodal decomposition occurs is still uncertain. Second, the free energy model in this work is based on a simple Landau free energy expansion. It seems rather difficult to adjust the coefficients for obtaining a wider composition range of spinodal decomposition in the t' -phase. In principle, if the width of the spinodal region determined by experiments is correct, other free energy models can be used. For example, a free energy model can be fitted to the schematic plot of the free energies of the tetragonal and cubic phases as shown in Fig. 8(d). Note that Figs. 1 and 8(d) are obviously similar except for the difference in the composition ranges for spinodal decomposition. Therefore, using a different free energy model will not change the main predictions and conclusions of this paper regarding the three possible transformation sequences for a c-phase aged in the $c + t$ two-phase field.

VII. Conclusions

A Landau free energy model is proposed for the ZrO_2 - Y_2O_3 alloy, which provides a first-order $c \rightarrow t$ phase transformation, and therefore two separate free-energy curves for the t-phase and the c-phase. Our thermodynamic stability analysis and computer simulations predict the following three different transformation sequences for a c-phase aged within the $c + t$ two-phase field: (1) direct nucleation and growth of the equilibrium t-phase from the c-phase matrix; (2) formation of a metastable t' -phase followed by nucleation and growth of the equilibrium c-phase; and (3) formation of a transient t' -phase followed by its spinodal decomposition into two tetragonal phases with one of the tetragonal phases eventually transforming to the equilibrium c-phase. This model seems to

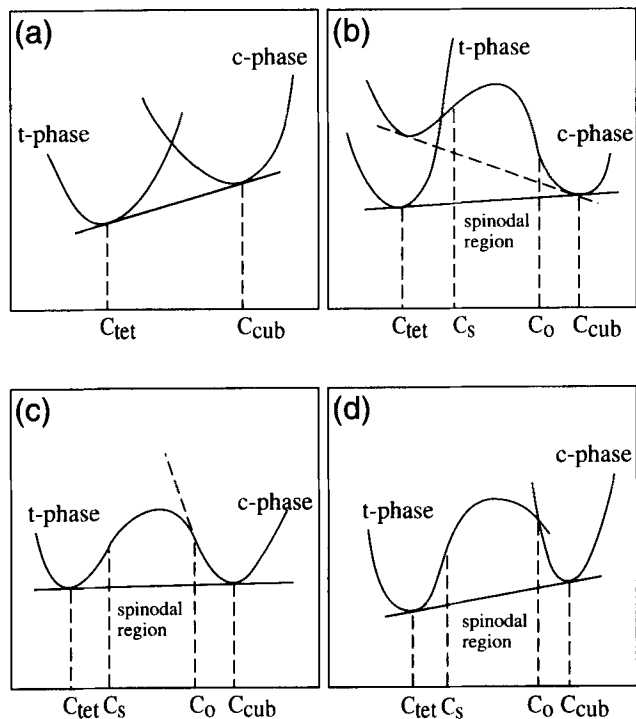


Fig. 8. Schematic free-energy vs composition curves for both the cubic and tetragonal phases: (a) Heuer *et al.* model (Ref. 3); (b,c) Sakuma *et al.* models (Ref. 12); (d) present model.

explain essentially all the existing experimental observations. The microstructure evolution during spinodal decomposition of the t' -phase predicted by our computer simulations has a striking resemblance to those observed experimentally.

Acknowledgments: We thank Mr. Y. Z. Wang, Professor A. G. Khachatryan, Professor V. S. Stubican, and Professor M. Doi for useful discussions. The computer simulations were performed on the Cray-90 at the Pittsburgh Supercomputing Center.

References

- ¹A. H. Heuer, "Transformation Toughening in ZrO₂-Containing Ceramics," *J. Am. Ceram. Soc.*, **70**, 689 (1987).
- ²W. R. Cannon, "Transformation Toughened Ceramics for Structural Applications," *Treatise Mater. Sci. Technol.*, **29**, 195 (1989).
- ³(a) A. H. Heuer, R. Chaim, and V. Lanteri, "Review: Phase Transformation and Microstructural Characterization of Alloys in the System Y₂O₃-ZrO₂," pp. 3–20 in *Advances in Ceramics*, Vol. 24, *Science and Technology of Zirconia III*. Edited by S. Somiya, N. Yamamoto, and H. Yanagida. American Ceramic Society, Westerville, OH, 1988. (b) A. H. Heuer, R. Chaim, and V. Lanteri, "The Displacive Cubic → Tetragonal Transformation in ZrO₂ Alloys," *Acta Metall.*, **35** [3] 661 (1987).
- ⁴D. L. Porter, A. G. Evans, and A. H. Heuer, "Transformation-Toughening in Partially-Stabilized Zirconia (PSZ)," *Acta Metall.*, **27**, 1649 (1979).
- ⁵C. A. Bateman and M. R. Notis, "Coherent Effects during Precipitate Coarsening in Partially Stabilized Zirconias," *Acta Metall. Mater.*, **40**, 2413 (1992).
- ⁶V. Lanteri, T. E. Mitchell, and A. H. Heuer, "Morphology of Tetragonal Precipitates in Partially Stabilized ZrO₂," *J. Am. Ceram. Soc.*, **70**, 564 (1986).
- ⁷V. S. Stubican, "Phase Equilibria and Metastabilities in the Systems ZrO₂-MgO, ZrO₂-CaO, and ZrO₂-Y₂O₃," pp. 71–82 in *Advances in Ceramics*, Vol. 24A, *Science and Technology of Zirconia III*. Edited by S. Somiya, N. Yamamoto, and H. Yanagida. American Ceramic Society, Westerville, OH, 1988.
- ⁸V. Lanteri, R. Chaim, and A. H. Heuer, "On the Microstructures Resulting from the Diffusionless Cubic → Tetragonal Transformation in ZrO₂-Y₂O₃ Alloys," *J. Am. Ceram. Soc.*, **69**, C-258 (1986).
- ⁹A. H. Heuer, R. Chaim, and V. Lanteri, "The Displacive Cubic → Tetragonal Transformation in ZrO₂ Alloys," *Acta Metall.*, **35**, 661 (1987).
- ¹⁰M. Doi and T. Miyazaki, "On the Spinodal Decomposition in Zirconia-Yttria (ZrO₂-Y₂O₃) Alloys," *Philos. Mag. B*, **68**, 305 (1993).
- ¹¹T. Sakuma, Y. I. Yoshizawa, and H. Suto, "The Modulated Structure Formed by Isothermal Aging in ZrO₂-5.2 mol% Y₂O₃ Alloy," *J. Mater. Sci.*, **20**, 1085 (1985).
- ¹²T. Sakuma, Y. I. Yoshizawa, and H. Suto, "The Metastable Two-Phase Region in the Zirconia-Rich Part of the ZrO₂-Y₂O₃ Alloy," *J. Mater. Sci.*, **21**, 1436 (1986).
- ¹³T. Sakuma, "Phase Transformation and Microstructure of Partially-Stabilized Zirconia," *Trans. Jpn. Inst. Met.*, **29**, 879 (1988).
- ¹⁴B. Bender, R. W. Rice, and J. R. Spann, "Precipitate Character in Laser-Melted PSZ," *J. Mater. Sci. Lett.*, **4**, 1331 (1985).
- ¹⁵M. Hillert, "Thermodynamic Model of the Cubic → Tetragonal Transition in Nonstoichiometric Zirconia," *J. Am. Ceram. Soc.*, **74**, 2005 (1991).
- ¹⁶M. Hillert and T. Sakuma, "Thermodynamic Modeling of the $c \rightarrow t$ Transformation in ZrO₂ Alloys," *Acta Metall. Mater.*, **39**, 1111 (1991).
- ¹⁷S. M. Allen and J. W. Cahn, "Mechanism of Phase Transformations within the Miscibility Gap of Fe-rich Fe-Al Alloys," *Acta Metall.*, **24**, 425 (1976).
- ¹⁸A. G. Khachatryan, T. F. Lindsey, and J. W. Morris, "Theoretical Investigation of the Precipitation of the δ' Phase in Al-Li," *Metall. Trans.*, **19**, 249 (1988).
- ¹⁹W. A. Soffa and D. E. Laughlin, "Decomposition and Ordering Processes Involving Thermodynamically First-Order Order → Disorder Transformations," *Acta Metall.*, **37**, 3019 (1989).
- ²⁰A. Onuki, "Ginzburg-Landau Approach to Elastic Effects in the Phase Separation of Solids," *J. Phys. Soc. Jpn.*, **58**, 3065 (1989).
- ²¹Y. Z. Wang, H. Y. Wang, L. Q. Chen, and A. G. Khachatryan, "Shape Evolution of a Coherent Tetragonal Precipitate in Partially Stabilized Cubic ZrO₂: A Computer Simulation," *J. Am. Ceram. Soc.*, **76**, 3029 (1993).
- ²²Y. Z. Wang, H. Y. Wang, L. Q. Chen, and A. G. Khachatryan, "Ginzburg-Landau Approach to Characterization of Kinetics of Coherent Structural Transformation with Symmetry Reduction: Decomposition in ZrO₂," *J. Am. Ceram. Soc.*, in press.
- ²³D. N. Fan and L.-Q. Chen, "Computer Simulation of Twin Formation during the Displacive $c \rightarrow t'$ Phase Transformation in the Zirconia-Yttria System," *J. Am. Ceram. Soc.*, **78** [3] 769–73 (1995).
- ²⁴J. W. Cahn and J. E. Hilliard, "Free Energy of a Nonuniform System. I. Interfacial Free Energy," *J. Chem. Phys.*, **28**, 258 (1958).
- ²⁵S. M. Allen and J. W. Cahn, "A Microscopic Theory for Antiphase Boundary Motion and Its Application to Antiphase Domain Coarsening," *Acta Metall.*, **27**, 1085 (1979).
- ²⁶A. G. Khachatryan and G. A. Shatalov, "Elastic-Interaction Potential of Defects in a Crystal," *Sov. Phys.—Solid State (Engl. Transl.)*, **11**, 118 (1969).
- ²⁷A. G. Khachatryan, "Some Questions Concerning the Theory of Phase Transformations in Solid," *Sov. Phys.—Solid State (Engl. Transl.)*, **8**, 2163 (1967). See also the monograph by A. G. Khachatryan, *Theory of Structural Transformations in Solids*; pp. 198–212. Wiley, New York, 1983. □